

# White and gray matter alterations in adults with Niemann-Pick disease type C

A cross-sectional study



M. Walterfang,  
FRANZCP  
M. Fahey, PhD, FRACP  
P. Desmond, MD,  
FRACR  
A. Wood, PhD  
M.L. Seal, PhD  
C. Steward, PhD  
C. Adamson, PhD  
C. Kokkinos, BAppSci  
M. Fietz, PhD  
D. Velakoulis,  
FRANZCP

Address correspondence and reprint requests to Dr. Mark Walterfang, Level 2, John Cade Building, Royal Melbourne Hospital, 3050 Melbourne, Australia  
mark.walterfang@mh.org.au

## ABSTRACT

**Objective:** Niemann-Pick disease type C (NPC) is a progressive neurovisceral disorder with disrupted intracellular cholesterol metabolism that results in significant alterations to neuronal and axonal structure. Adult patients present with ataxia, gaze palsy, impaired cognition, and neuropsychiatric illness, but the neural substrate has not been well-characterized in vivo. Our aim was to investigate a well-characterized sample of adults with confirmed NPC for gray and white matter abnormalities.

**Methods:** We utilized a combination of optimized voxel-based morphometry of T1-weighted images and tract-based spatial statistics of diffusion tensor images to examine gray matter volume and white matter structural differences in 6 adult patients with NPC and 18 gender- and age-matched controls.

**Results:** Patients with NPC demonstrated bilateral gray matter reductions in large clusters in bilateral hippocampus, thalamus, superior cerebellum, and insula, in addition to smaller regions of inferoposterior cortex. Patients demonstrated widespread reductions in fractional anisotropy in major white matter tracts. Subsequent analysis of measures of axial and radial diffusivity suggest that these changes are contributed to by both impaired myelination and altered axonal structure.

**Conclusions:** Findings in gray matter areas are broadly consistent with human and animal studies of selective vulnerability of neuronal populations to the neuropathology of NPC, whereas more widespread white matter changes are consistent with the hypothesis that disrupted myelination and axonal structure predate changes to the neuronal cell body. These findings suggest that volumetric analysis of gray matter and diffusion tensor imaging may be useful modalities for indexing illness stage and monitoring response to emerging treatment. *Neurology*® 2010;75:49-56

## GLOSSARY

**DTI** = diffusion tensor imaging; **FA** = fractional anisotropy; **MD** = mean diffusivity; **NFT** = neurofibrillary tangle; **NPC** = Niemann-Pick disease type C; **RD** = radial diffusivity; **TBSS** = tract-based spatial statistics; **TE** = echo time; **TR** = repetition time.

Niemann-Pick disease type C (NPC) is a progressive neurovisceral disorder of intracellular sterol cycling that results from mutations to the genes encoding for the NPC1 and NPC2 proteins, and presents in adults in 10%–20% of cases.<sup>1</sup> This results in splenomegaly, ataxia, vertical supranuclear ophthalmoplegia, and cognitive impairment.<sup>2</sup> Adult-onset presentations are often associated with significant neuropsychiatric disturbance, particularly schizophrenia-like psychosis.<sup>3</sup>

The effects of accumulation of cholesterol and glycolipids on neural tissue are wide-ranging and affect dendritic and axonal morphology, alter axonal transport and intracellular lysosomal transport, and affect neuronal–glial interactions.<sup>4</sup> GM2 and GM3 gangliosides, glucosylceramide, and lactosyl ceramide are accumulated in both white and gray matter.<sup>5</sup> This results in

Supplemental data at  
[www.neurology.org](http://www.neurology.org)

*e-Pub ahead of print on May 19, 2010, at [www.neurology.org](http://www.neurology.org).*

From the Melbourne Neuropsychiatry Centre & Department of Psychiatry (M.W., M.L.S., D.V.), University of Melbourne and North Western Mental Health Program, Sunshine Hospital and Royal Melbourne Hospital, Melbourne; Department of Paediatrics (M. Fahey), Monash University, Melbourne; Department of Radiology (P.D., C.S., C.K.), Royal Melbourne Hospital, Melbourne; Murdoch Childrens Research Institute (A.W., C.A.), Royal Children's Hospital, Melbourne; Department of Radiology (P.D., C.S.), University of Melbourne, Melbourne; SA Pathology (M. Fietz), Women's and Children's Hospital, Adelaide; and School of Molecular and Biomedical Science (M. Fietz), University of Adelaide, Adelaide, Australia.

*Study funding:* Supported by a Pfizer Neuroscience Research Grant (to M.W.).

*Disclosure:* Author disclosures are provided at the end of the article.

significant ultrastructural change to neuronal cell bodies, axons, and dendrites that is associated with significant axonal and neuronal loss.<sup>4,6</sup> Modern neuroimaging techniques such as MRI can allow for the assessment and monitoring of these changes in vivo, although the relative rarity of adult NPC has meant that few systematic studies have been undertaken. However, no systematic studies have examined regional gray matter changes in patients with NPC to determine if neuroimaging changes match the distribution of the neuropathologic changes reported from animal and human postmortem studies.

We utilized a well-characterized adult NPC cohort and compared them in a cross-sectional design against age- and gender-matched controls to explore gray and white matter changes, and hypothesized that we would see significant widespread cortical atrophy, particularly in frontal zones, and widespread disruption to white matter microstructure.

**METHODS** **Standard protocol approval, registration, and patient consent.** All participants provided written informed consent and the study was approved by the local research and ethics committee (HREC 2004.042 and 2005.198).

**Subjects.** Data were acquired from 6 adult patients with NPC (4 male, 2 female), all from the Royal Melbourne Hospital, Australia (table 1), between 2007 and 2009. All adult patients with NPC assessed during this period were included. Diagnosis was confirmed with biochemical analysis of cultured fibroblasts, using cholesterol esterification rate and percentage of cells staining abnormally for perinuclear cholesterol. Patients were matched 3-for-1 for age and gender with healthy controls (n = 18; 11 male, 7 female) without a history of major medical, neurologic, or psychiatric illness, and the study was approved by the local research and ethics committee.

**MRI acquisition.** All subjects were scanned on a 1.5-T GE Signa MRI machine at the Royal Melbourne Hospital. A volumetric spoiled gradient recalled echo sequence generated 124 contiguous, 1.5-mm coronal slices with echo time (TE)/repetition time (TR) 3.3/14.3 msec; flip angle, 30°; matrix size, 256 × 256; field of view, 24 × 24 cm; voxel dimensions, 0.938 × 0.938 mm. Diffusion tensor imaging (DTI) was undertaken via a 25-direction (one b0 image) echoplanar imaging sequence with 20 axial 5-mm slices, b-value of 1,000; TE/TR 90/6,000 msec; flip angle, 90°; matrix size, 256 × 256; voxel dimensions, 0.938 × 0.938 mm. A numerical code was used to ensure blind analysis of data.

**White matter preprocessing.** Maps of fractional anisotropy (FA), mean diffusivity (MD), axial diffusivity ( $\lambda_{\parallel} = \lambda_1$ , the first eigenvalue), and radial diffusivity (RD, or  $\lambda_{\perp} = \lambda_{2,3}$ , the average of the second and third eigenvalues) were generated using the FMRIB Diffusion Toolbox, part of the FSL software package,

**Table 1** Demographic and illness details on adult patients with Niemann-Pick disease type C at initial presentation and time of scanning

| Patient | Age at scan, y | Gender | Illness duration, y | Initial clinical presentation                       | VSO | Dystonia | Ataxia | Dysarthria | Filipin staining, % | Cholesterol esterification rate, pmol/h/mg | Illness rating | MMSE score | Full-scale IQ (scaled) |
|---------|----------------|--------|---------------------|---|-----|----------|--------|------------|---------------------|--|----------------|------------|------------------------|
| 1       | 32             | F      | 5                   | Psychosis, VSO                                      | ++  | +        | +      | +          | 50-60               | 5.3  | 7              | 30         | 70                     |
| 2       | 32             | M      | 16                  | P-schosis, VSO, ataxia, dysarthria                  | +++ | ++       | +++    | ++         | 60-70               | 2.9  | 11             | 20         | 66                     |
| 3       | 31             | M      | 13                  | Psychosis, VSO, ataxia                              | +++ | ++       | ++     | +++        | 95-100              | 0.3  | 15             | 15         | 65                     |
| 4       | 18             | M      | 5                   | VSO, ataxia, dysarthria                             | +   | -        | +      | +          | 80                  | 1.3  | 7              | 22         | 75                     |
| 5       | 20             | M      | 3                   | Dysexecutive syndrome, mild ataxia, mild dysarthria | +   | +        | ++     | ++         | 95-100              | 2.0  | 5              | 27         | 76                     |
| 6       | 33             | F      | 5                   | Dysexecutive syndrome, ataxia, dysarthria           | ++  | +        | +      | +          | 25                  | 1.5  | 9              | 13         | 55                     |

Abbreviations: MMSE = Mini-Mental State Examination, score out of 30; VSO = vertical supranuclear ophthalmoplegia.

version 4.1.4.<sup>7</sup> In order to minimize potential false-positive findings caused by misregistration of disease-related morphologic changes in gray and white matter in the NPC group, voxel-wise statistical analysis of the FA data was carried out using tract-based spatial statistics (TBSS),<sup>8</sup> also part of the FSL package.<sup>7</sup> FA images were created by fitting a tensor model to the raw diffusion data using FDT,<sup>7</sup> and the brain extracted using brain extraction tool. All subjects' FA data were then aligned into common space using the nonlinear registration tool FNIRT. Next, the mean FA image was created and thinned to create a mean FA skeleton, which represents the centers of all tracts common to the group. Each subject's aligned FA data were then projected onto this skeleton, to remove the effect of cross-subject spatial variability that remains after the nonlinear registration, and resulting data fed into voxel-wise cross-subject statistics. Subsequently, other relevant DTI output images (MD, axial diffusivity, RD) were projected onto the mean FA skeleton so other diffusivity values could be compared between groups in the same spatial location.

**Gray matter preprocessing.** Structural data were analyzed with FSL-VBM, a voxel-based analysis carried out with FSL tools.<sup>7</sup> Structural images were brain-extracted and tissue-type segmentation was carried out using FAST4 from the FSL package. Resulting gray-matter partial volume images were then aligned to MNI152 standard space using the affine registration tool FLIRT,<sup>9</sup> followed by nonlinear registration using FNIRT. Resulting images were averaged to create a study-specific template, to which native gray matter images were then nonlinearly reregistered. Registered partial volume images were then modu-

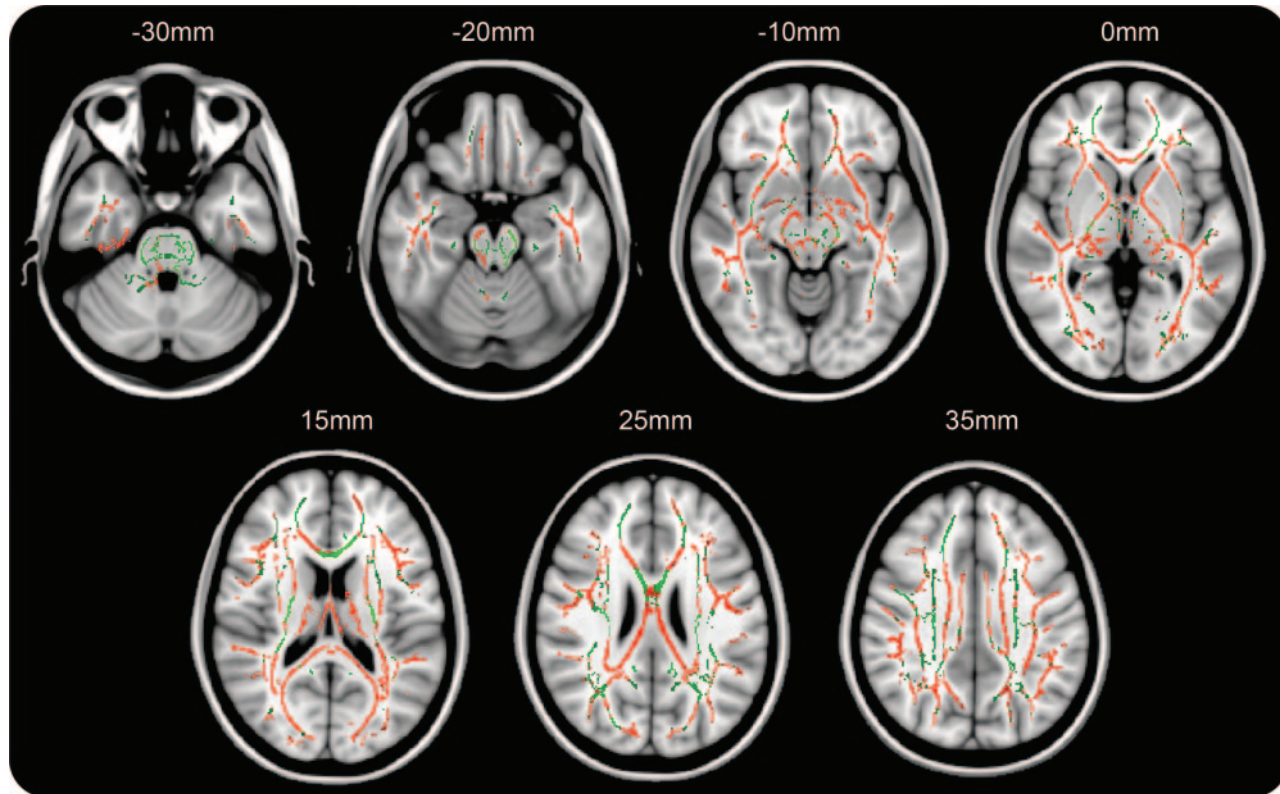
lated (to correct for local expansion or contraction) by dividing by the Jacobian of the warp field. The modulated segmented images were then smoothed with an isotropic Gaussian kernel with a sigma of 3 mm.

**Statistical analyses.** Between-group analyses were conducted using Randomize, a permutation-based nonparametric analysis program from the FSL package. We used permutation-based nonparametric inference within the framework of the general linear model to investigate changes in the gray matter, FA, MD, RD, and axial diffusivity between both groups, with threshold-free cluster enhancement with 5,000 permutations per analysis. Reported results are robust clusters corrected for multiple comparisons across space ( $p < 0.05$  corrected).

**RESULTS** There was no difference between the patient groups in gender ratio ( $\chi^2 = 0.06$ ,  $p = 0.81$ ) or age [mean age NPC group,  $27.67 \pm 6.78$ , control group  $26.28 \pm 4.56$ ;  $t(23) = 0.47$ ,  $p = 0.65$ ].

**White matter results.** Results from TBSS mapping of differences in FA between patients with NPC and controls demonstrated widespread reductions in the patient group bilaterally, affecting most brain regions and projection as well as association fibers (figure 1). There were no regions of increased FA relative to controls. In MD maps, we found significant wide-

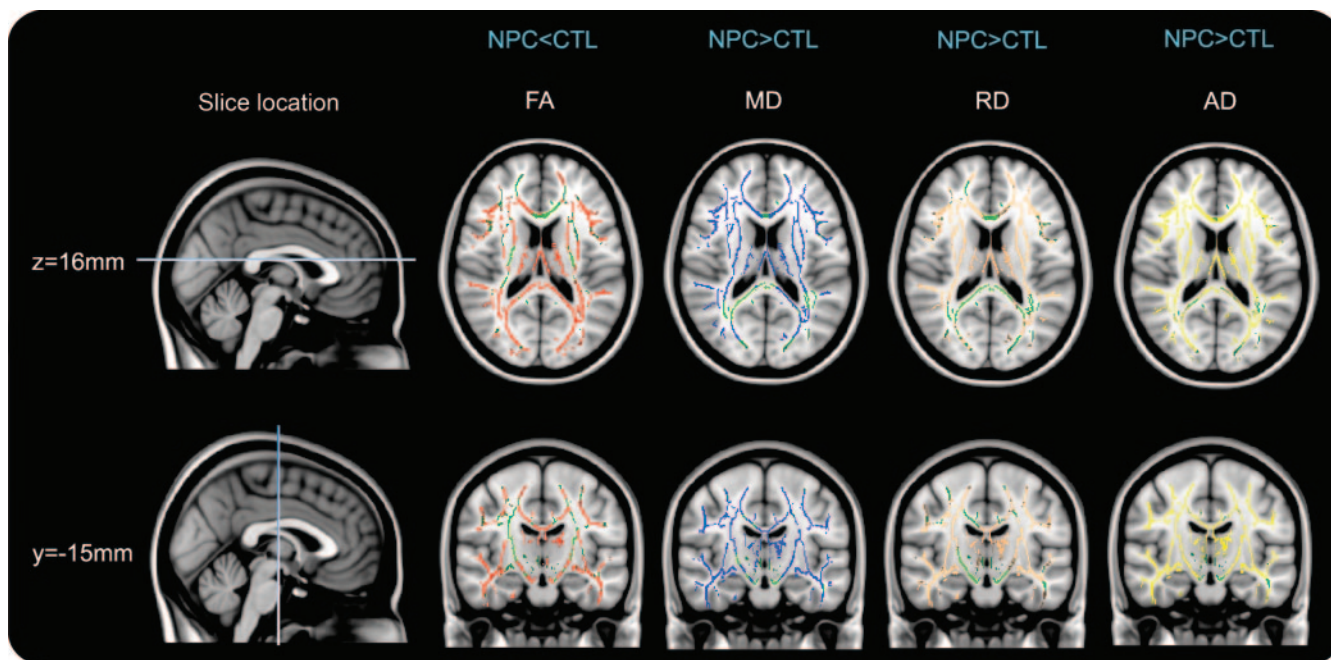
**Figure 1** Changes in white matter fractional anisotropy



Results of tract-based spatial statistics voxel-wise analysis for fractional anisotropy (FA). Results are shown on the MNI152 1-mm template, with the mean FA skeleton common to all subjects shown in green. Areas of significant FA reduction in the Niemann-Pick disease type C group are shown in red, and represent cluster-based values ( $p < 0.05$ , corrected). Montreal Neurological Institute space z-axis coordinates are provided in mm. Images presented in radiologic format.



**Figure 2** Comparison of white matter anisotropy and diffusivity



Results of tract-based spatial statistics voxel-wise analysis showing regions of between-group differences in fractional anisotropy (FA), mean diffusivity (MD), radial diffusivity (RD), and axial diffusivity (AD). Results are shown on the MNI152 1-mm template, with the mean FA skeleton common to all subjects shown in green. Areas of significant FA reduction in the Niemann-Pick disease type C group are shown in red, MD increases in blue, RD increases in orange, and AD increases in yellow, and represent cluster-based values ( $p < 0.05$ , corrected). Montreal Neurological Institute space z-axis and y-axis coordinates are provided in mm. Images presented in radiologic format. CTL = control.

spread increases that corresponded to regions of FA reduction. Separating diffusivity into its axial (axial diffusivity) and radial (RD) components showed that each was significantly increased in the NPC group (figure 2). Significant clusters were localized using the Johns Hopkins white matter atlas within FSL-View 3.1.2. Mean values for FA, MD, RD, and axial diffusivity for representative white matter regions, using region-of-interest masks from the Johns Hopkins atlas on the common TBSS skeleton for patients and controls, are shown in table e-1 on the *Neurology*<sup>®</sup> Web site at [www.neurology.org](http://www.neurology.org).

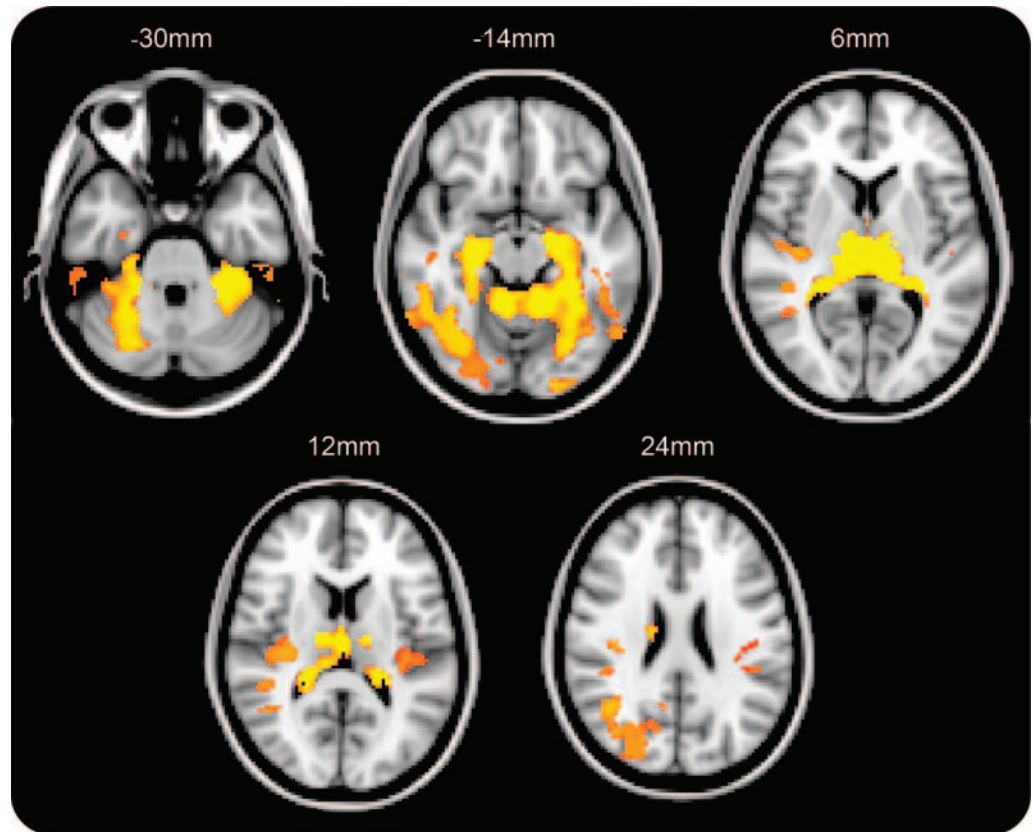
**Gray matter results.** Voxel-based comparison of patients with NPC revealed bilateral and highly significant differences in gray matter volume distribution (patients < controls) in the planum temporale, Heschl gyrus, and parietal operculum; left and right hippocampus and parahippocampal gyrus; left and right thalamus; right putamen; and anterior/superior cerebellar lobules I–VI (figures 3 and 4). There were no regions of significant increases in gray matter volume. Significant clusters were localized using the Harvard-Oxford cortical and subcortical atlases, and the MNI152 cerebellar atlases, within FSL-View.

**DISCUSSION** In a well-characterized sample of adult patients with NPC, we found widespread alterations to

white matter microstructure and focal changes in gray matter volume. Our study is the first systematic study of adult patients with NPC that specifically examined gray matter volume in comparison to a control group, and the first to use a whole-brain approach. While DTI has shown promise as a marker of CNS pathology in animal models and as a mechanism to detect change, no statistical analyses of white matter microstructure have previously been undertaken in NPC.

We predicted widespread changes in gray matter regions, as has previously been reported in a number of case reports and series in adults, although the presence of such gray matter changes is far from universal and tends to be most apparent late in the illness course.<sup>3,10,11</sup> Neocortical regions were generally spared from volumetric change, except for the inferior temporal gyrus, planum temporale, and parietal operculum. The strongest bilateral findings occurred in the insular cortex, hippocampal and parahippocampal regions, bilateral superior cerebellum, thalamic gray matter, and to a lesser extent the striatum. These findings suggest a particular pattern of gray matter volumetric change that may reflect differential vulnerability of certain neuronal populations to the neuropathology of NPC, which may be more apparent in adult patients with NPC due to the less fulminant biochemical disruption and illness course in adults.

**Figure 3** Change in gray matter volume

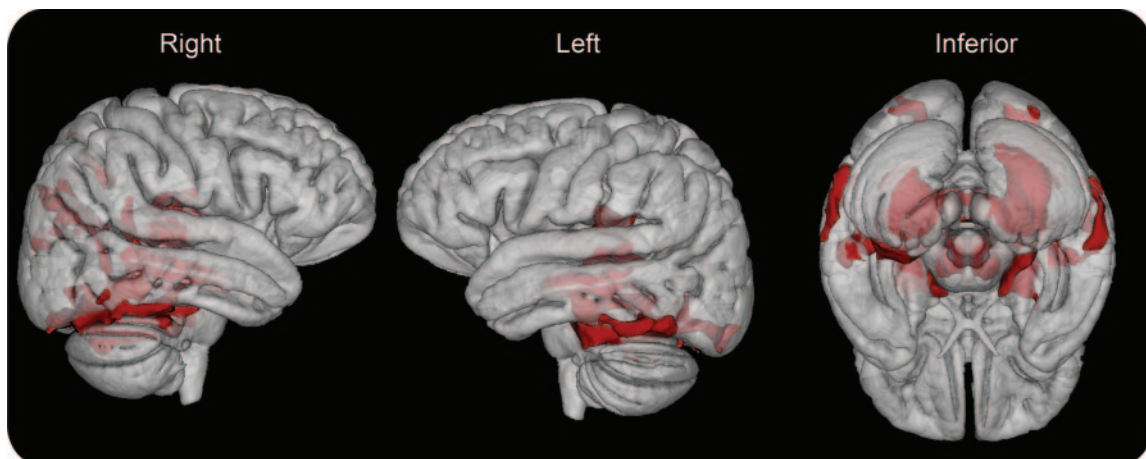


Results of FSL-VBM voxel-wise analysis showing regions of between-group differences in gray matter volume, with all regions representing volume loss in the Niemann-Pick disease type C group compared to controls. Results are shown on the MNI152 2-mm template, with significant voxels shown on a red-yellow significance spectrum (from  $p < 0.05$  to 0) and representing cluster-based values. Montreal Neurological Institute space z-axis coordinates are provided in mm. Images presented in radiologic format.

The reasons for the apparent selective vulnerability of neurons in NPC remain unclear, although animal NPC1 models have been revealing.<sup>6</sup> In NPC1

cats, while abnormal storage products occur in neurons across the CNS, only cerebellar Purkinje neurons are completely lost,<sup>12</sup> suggesting these are the

**Figure 4** Three-dimensional projection of gray matter volume changes



Results of FSL-VBM voxel-wise analysis represented in 3 dimensions on the MNI152 2-mm template. Left and right views show changes in inferior temporal gyrus and insular/planum temporale region, and inferior view shows changes in superior cerebellar and medial temporal regions.

most susceptible. Additionally, while GM2 ganglioside storage varies across cell populations, those cell populations with greatest storage of GM2 are associated with characteristic ectopic dendritic sprouting.<sup>13</sup> Finally, cats with NPC1 disease have been shown to only exhibit axonal spheroids in GABAergic neuronal populations, including cerebellum, brainstem, cerebral cortex (including hippocampus), and basal ganglia.<sup>14</sup> Significant axonal spheroid formation, which occurs in a range of storage disorders, appears to be necessary for clinical neurologic disease.<sup>12</sup> In NPC1 and NPC2 mouse models, intracellular storage of GM2 and GM3 gangliosides is conspicuous in Purkinje cells, large pyramidal neurons, and neurons in the lateral thalamus, hippocampus, and brainstem.<sup>15-17</sup> In NPC mice, neuronal loss occurs in the cerebellum, as in cats, and Purkinje cells in the cerebellum deteriorate in a stepwise fashion, with neurons in lobules IX and X in the posterior vermis surviving longest.<sup>18</sup> Additionally, significant neuronal loss occurs in the murine thalamus.<sup>16,19</sup> Finally, one pathology not reported in animal models, but described in human postmortem samples, is the formation of neurofibrillary tangles (NFTs) in basal ganglia, brainstem, cerebral cortex, and hippocampus (particularly CA1 and CA2),<sup>20-22</sup> but not in cerebellar Purkinje cells.<sup>23</sup> This suggests that the combination of regional ganglioside excess driving altered neuronal morphology and/or loss in the cerebellum, hippocampus, brainstem, thalamus, and cortex may interact with further ultrastructural changes (via altered microtubular function) leading to NFT accumulation in many of the same regions. Overall, our findings in gray matter marry well with these neuropathologic findings from these disparate models, supporting the validity of our findings.

In contrast to relatively selective gray matter findings, white matter changes affected most major tracts. Few studies have probed white matter integrity directly in NPC. Galanaud et al.<sup>24</sup> reported similar baseline alterations in centrum semiovale NAA/Cre in adult NPC, and an attenuation of abnormal Cho/Cre levels following 24 months' treatment with the substrate reduction therapy miglustat. One report of a pediatric patient with NPC utilized DTI, which indexes the integrity of white matter microstructure. In animal NPC models, DTI has demonstrated reductions in white matter integrity in NPC mice compared to wild-type mice, partially reversible with neurosteroid or cyclodextrin treatment,<sup>25</sup> suggesting it may be a useful biomarker of illness status and treatment response. One report of a pediatric patient with NPC demonstrated marked global reductions in white matter integrity, particularly in the corpus callosum.<sup>26</sup>

Despite the widespread use of DTI as a neuroimaging tool to probe illness progression in a range of neurologic disorders, it has not been utilized in adult NPC samples. Alterations in measures such as FA may reflect changes at the level of the axon, or in oligodendrocytes and their investing myelin sheath. There is significant evidence of alterations to axonal structure in NPC, including focal axonal swelling and spheroids, in addition to abnormal axonal branching and the formation of recurrent axonal collaterals.<sup>12,17,27</sup> Reduced axonal number may also occur in long association or commissural tracts such as the corpus callosum.<sup>28</sup> This may be the result of reduced transport of cholesterol to distal axons, limiting their growth.<sup>29</sup> Myelination is also severely disrupted, with reduction of myelin-specific proteins suggestive of reduced myelination, rather than destruction of normally formed myelin.<sup>28,30</sup> In an NPC mouse model, normal myelination was differentially disrupted, being particularly reduced across the callosum, but relatively intact in internal capsules, cerebellar white matter, brainstem, and spinal cord,<sup>31</sup> areas less affected in our study. There is evidence from murine NPC models that reduced myelination is underpinned by reduced differentiation of, and abnormal inclusions within, oligodendrocytes.<sup>32</sup> This suggests a more widespread early pattern of white matter change due to the combination of altered axonal structure and reduced myelination, with a relative sparing of basal white matter structures. This is consistent with our findings of widespread reduction in FA, which may be the result of perturbed axonal structure and organization, and reduced myelination.<sup>33</sup> The increases in radial diffusivity in most regions suggest widespread dysmyelination,<sup>34</sup> while altered axial diffusivity suggests axonal degeneration and/or reorganization,<sup>35</sup> consistent with the neuropathologic models of white matter alterations in NPC.

Most reductions in gray matter were associated with surrounding perturbations to white matter tracts. This may reflect a differential effect of NPC neuropathology on gray and white matter compartments, or it may reflect a relatively early alteration to white matter fiber and sheath structure in NPC, with gray matter changes occurring later. This is supported by a murine NPC model, with evidence that axons are the first affected structures in NPC, with neuronal cell bodies showing much later degeneration,<sup>36</sup> although it should be noted that white matter pathology may be more severe in the Balb/c murine model than in humans and this may partially account for this differential effect. The only *in vivo* way to confirm this would be through longitudinal neuroimaging analysis. However, we note that our gray



matter analysis was volumetric rather than microstructural, and while these measures are related, they do not necessarily change collinearly. As a result, it is possible that a method that focuses on volume distribution of gray matter may fail to detect more widespread microstructural changes that are yet to manifest in gray matter change.

These imaging changes correlate with clinical findings in adults with NPC. Adult patients generally present with ataxia and dystonia,<sup>10</sup> which may relate to cerebellar and striatal changes. While the degree and pattern of neuropsychological impairment may vary considerably in adult patients with NPC,<sup>10,37,38</sup> the strong bilateral reductions in hippocampal volume are consistent with the often significant verbal working memory deficits described.<sup>37</sup> However, significant executive disturbance is also described, and we did not demonstrate volumetric changes to frontal cortex in our study, although executive changes could be attributable to superomedial cerebellar alterations. Additionally, the characteristic vertical supranuclear ophthalmoplegia is not reflected in significant brainstem changes in gray and white matter, although the limited resolution of traditional MRI at 1.5-T field strength in this brain region may limit the capacity of registration-dependent, voxel-based approaches to detect change, particularly DTI.<sup>39</sup> However, given that a disproportionate number of adult patients with NPC present with schizophrenia-like psychosis,<sup>3,11</sup> it is notable that we have shown widespread evidence of anatomic disconnectivity via altered white matter structure in adult NPC, which has been posited as the substrate of the functional disconnectivity believed to underpin schizophrenic symptoms. Furthermore, a number of the gray matter regions in our study—most particularly, the medial temporal lobe, but also including the thalamus and cerebellum—have been strongly implicated in the neuropathology of schizophrenia. Adult NPC, like a number of other adult-onset neurometabolic disorders, may present with a schizophrenia-like presentation due to the combination of anatomic disconnectivity and disruption to gray matter structures that play a crucial role in integrating information from higher cortical centers.

This study is affected by a number of limitations. Although this is the first study of its type in this disorder, the sample size of affected adult patients with NPC is small because of the rarity of the disorder. This may limit the generalization of our results to the adult NPC population. The small sample may also limit the power to detect between-group differences, particularly when using a methodologically and statistically conservative neuroimaging analysis. We attempted to mitigate this with a larger matched

control sample. In spite of this, we detected widespread changes in white matter structure and a number of changes in gray matter regions. Additionally, while we are examining nonvolumetric microstructural changes in white matter, our methodology limits the assessment of gray matter to volume changes alone, and does not probe cortical microstructural changes. This may limit the comparability of our gray and white matter findings, and future studies using microstructural methodologies that assess both white and gray matter (such as magnetization transfer imaging) may resolve this. Further elucidation of the relationship between gray and white matter changes requires longitudinal imaging across the illness lifespan. Our findings suggest that neuroimaging measures can provide a neurobiologic marker of illness status, which—as in animal NPC models—may provide a means for indexing the disease response to emerging treatments in human patients with NPC.

## DISCLOSURE

Dr. Walterfang has served on a scientific advisory board and as a consultant for and received funding for travel from Actelion Pharmaceuticals Ltd. and received royalties from the publication of *Kaplan and Sadock's Comprehensive Textbook of Psychiatry* (Lippincott Williams & Wilkins, 2009). Dr. Fahey has served on a scientific advisory board and as a consultant for and received funding for travel from Actelion Pharmaceuticals Ltd.; has received speaker honoraria from the Australian Podiatry Association; receives research support from NHMRC and the NIH (1R03HD058625-01, CI); has held/holds stock in Sigma Pharmaceuticals, LLC, and Peplin, Inc.; and has given expert testimony on behalf of the Therapeutic Goods Administration. Dr. Desmond serves on the editorial board of the *Journal of Clinical Neuroscience* and as an Associate Editor of the *Journal of Medical Imaging and Radiation Oncology* and receives research support from NHMRC, Cancer Australia, the National Health Foundation, and The Royal Melbourne Hospital Neuroscience Foundation. Dr. Wood has received research support from the Australian Research Council and Australian Rotary Health. Dr. Seal has received fellowship support from the University of Melbourne (Ronald Phillip Griffith Fellowship) and research support from NHMRC. Dr. Steward, Dr. Adamson, and Dr. Kokkinos report no disclosures. Dr. Fietz has served on a scientific advisory board for Actelion Pharmaceuticals Ltd. and has received funding for travel from Genzyme Corporation and Actelion Pharmaceuticals Ltd. Dr. Velakoulis has received royalties from the publication of *Kaplan and Sadock's Comprehensive Textbook of Psychiatry* (Lippincott Williams & Wilkins, 2009).

Received November 21, 2009. Accepted in final form February 23, 2010.

## REFERENCES

1. Vanier M, Millat G. Niemann-Pick disease type C. *Clin Genet* 2003;64:269–281.
2. Patterson M, Vanier M, Suzuki K, et al. Niemann-Pick disease type C: a lipid trafficking disorder. In: Scriver C, Beaudet A, Sly W, et al., eds. *The Metabolic and Molecular Bases of Inherited Disease*. New York: McGraw Hill; 2001:3611–3634.
3. Walterfang M, Fietz M, Fahey M, et al. The neuropsychiatry of Niemann-Pick type C disease in adulthood. *J Neuropsychiatry Clin Neurosci* 2006;18:158–170.

4. Paul C, Boegle A, Maue R. Before the loss: neuronal dysfunction in Niemann-Pick type C disease. *Biochim Biophys Acta* 2004;1685:63–76.
5. Vanier M. Lipid changes in Niemann-Pick disease type C brain: personal experience and review of the literature. *Neurochem Res* 1999;24:481–489.
6. Walkley S, Suzuki K. Consequences of NPC1 and NPC2 loss of function in mammalian neurons. *Biochim Biophys Acta* 2004;1685:48–62.
7. Smith S, Jenkinson M, Woolrich M, et al. Advances in functional and structural MR image analysis and implementation as FSL. *Neuroimage* 2004;23:S208–S219.
8. Smith S, Jenkinson M, Johansen-Berg H, et al. Tract-based spatial statistics: voxel-wise analysis of multi-subject diffusion data. *Neuroimage* 2006;31:1487–1505.
9. Jenkinson M, Smith S. A global optimisation method for robust affine registration of brain images. *Med Image Anal* 2001;5:143–156.
10. Sevin M, Lesca G, Baumann M, et al. The adult form of Niemann-Pick disease type C. *Brain* 2007;130:120–133.
11. Josephs K, Van Gerpen M, Van Gerpen J. Adult-onset Niemann-Pick disease type C presenting with psychosis. *J Neurol Neurosurg Psychiatry* 2003;74:528–529.
12. March P, Thrall M, Brown D, et al. GABAergic neuroaxonal dystrophy and other cytopathological alterations in feline Niemann-Pick disease type C. *Acta Neuropathol* 1997;94:164–172.
13. Siegel D, Walkley S. Growth of ectopic dendrites on cortical pyramidal neurons in neuronal storage diseases correlates with abnormal accumulation of GM2 ganglioside. *J Neurochem* 1994;62:1852–1862.
14. Walkley S, Baker H, Rattazzi M, et al. Neuroaxonal dystrophy in neuronal storage disorders: evidence for major GABAergic neuron involvement. *J Neurol Sci* 1991;104:1–8.
15. Taniguchi M, Shinoda Y, Ninomiya H, et al. Site and temporal changes of gangliosides GM1/GM2 storage in the Niemann-Pick disease type C mouse brain. *Brain Dev* 2001;23:414–421.
16. German D, Quintero E, Liang C, et al. Selective neurodegeneration, without neurofibrillary tangles, in a mouse model of Niemann-Pick C disease. *J Comp Neurol* 2001;433:415–425.
17. Zervas M, Dobrenis K, Walkley S. Neurons in Niemann-Pick type C accumulate gangliosides as well as unesterified cholesterol and undergo dendritic and axonal alterations. *J Neuropathol Exp Neurol* 2001;60:49–64.
18. Higashi Y, Murayama S, Pentchev P, Suzuki K. Cerebellar degeneration in the Niemann-Pick type C mouse. *Acta Neuropathol* 1993;85:175–184.
19. Yamada A, Ukita M, Shinoda Y, et al. Progressive neuronal loss in the ventral posterior lateral and medial nuclei of thalamus in Niemann-Pick disease type C mouse brain. *Brain Dev* 2001;5:288–297.
20. Love S, Bridges L, Case C. Neurofibrillary tangles in Niemann-Pick disease type C. *Brain* 1995;118:119–129.
21. Suzuki K, Parker C, Pentchev P, et al. Neurofibrillary tangles in Niemann-Pick disease type C. *Acta Neuropathol* 1995;89:227–238.
22. Suzuki K, Parker C, Pentchev P. Niemann-Pick disease type C: neuropathology revisited. *Dev Brain Dysfunct* 1997;10:306–320.
23. Bu B, Klunemann H, Suzuki K, et al. Niemann-Pick type C yields possible clues for why cerebellar neurons do not form neurofibrillary tangles. *Neurobiol Dis* 2002;11:285–297.
24. Galanaud D, Tourbah A, Lehericy S, et al. 24 month treatment with miglustat of three patients with Niemann-Pick type C: follow up using brain spectroscopy. *Mol Genet Metab* 2009;96:55–58.
25. Lope-Piedrafita S, Totenhagen J, Hicks C, et al. MRI detects therapeutic effects in weanling Niemann-Pick type C mice. *J Neurosci Res* 2008;86:2802–2807.
26. Trouard T, Heidenreich R, Seeger J, Erickson R. Diffusion tensor imaging in Niemann-Pick type C disease. *Pediatr Neurol* 2005;33:325–330.
27. Sarna J, Larouche M, Marzban H, et al. Patterned Purkinje cell degeneration in mouse models of Niemann-Pick type C disease. *J Comp Neurol* 2003;456:279–291.
28. German D, Liang C, Song T, et al. Neurodegeneration in the Niemann-Pick C mouse: glial involvement. *Neurosci* 2002;109:437–450.
29. Karten B, Vance D, Campenot R, Vance J. Trafficking of cholesterol from cell bodies to distal axons in Niemann-Pick C1-deficient neurons. *J Biol Chem* 2003;278:4168–4175.
30. Goodrum J, Pentchev P. Cholesterol reutilization during myelination of regenerating PNS axons is impaired in Niemann-Pick disease type C mice. *J Neurosci Res* 1997;49:389–392.
31. Weintraub H, Abramovici A, Sandbank U, et al. Dysmyelination in NCTR-Balb/C mouse mutant with a lysosomal storage disorder: morphological survey. *Acta Neuropathol* 1987;74:374–381.
32. Takikita S, Fukuda T, Mohri I, et al. Perturbed myelination process of premyelinating oligodendrocyte in Niemann-Pick type C mouse. *J Neuropathol Exp Neurol* 2004;63:660–673.
33. Le Bihan D, Mangin J-F, Poupon C, et al. Diffusion tensor imaging: concepts and applications. *J Magn Reson Imaging* 2001;13:534–546.
34. Song S, Yoshino J, Le T, et al. Demyelination increases radial diffusivity in corpus callosum of mouse brain. *Neuroimage* 2005;26:132–140.
35. Song S, Sun S, Ju W, et al. Diffusion tensor imaging detects and differentiates axons and myelin degeneration in mouse optic nerve after retinal ischemia. *Neuroimage* 2003;20:1714–1722.
36. Ong W, Kumar U, Switzer R, et al. Neurodegeneration in Niemann-Pick type C disease mice. *Exp Brain Res* 2001;141:218–231.
37. Klarner B, Klunemann H, Lurding R, et al. Neuropsychological profile of adult patients with Niemann-Pick C1 (NPC1) mutations. *J Inher Metab Dis* 2007;30:60–67.
38. Hinton V, Vecchio D, Prady H, et al. The Cognitive Phenotype of Type C Disease: Neuropsychological Characteristics of Patients at Baseline in a Clinical Trial with Oral Miglustat. Salt Lake City: American Society of Human Genetics; 2005.
39. Yamada K, Shiga K, Kizu O, et al. Oculomotor nerve palsy evaluated by diffusion-tensor tractography. *Neuroradiology* 2006;48:434–437.



**White and gray matter alterations in adults with Niemann-Pick disease type C: A cross-sectional study**

M. Walterfang, M. Fahey, P. Desmond, A. Wood, M.L. Seal, C. Steward, C. Adamson, C. Kokkinos, M. Fietz and D. Velakoulis

*Neurology* 2010;75:49-56; originally published online May 19, 2010;

DOI: 10.1212/WNL.0b013e3181e6210e

**This information is current as of July 9, 2010**

|   |   |
|---|---|
| <b>Updated Information &amp; Services</b> | including high-resolution figures, can be found at:<br><a href="http://www.neurology.org/cgi/content/full/75/1/49">http://www.neurology.org/cgi/content/full/75/1/49</a>  |
| <b>Supplementary Material</b>             | Supplementary material can be found at:<br><a href="http://www.neurology.org/cgi/content/full/WNL.0b013e3181e6210e/DC1">http://www.neurology.org/cgi/content/full/WNL.0b013e3181e6210e/DC1</a>  |
| <b>Subspecialty Collections</b>           | This article, along with others on similar topics, appears in the following collection(s):<br><b>MRI</b><br><a href="http://www.neurology.org/cgi/collection/mri">http://www.neurology.org/cgi/collection/mri</a> <b>All Movement Disorders</b><br><a href="http://www.neurology.org/cgi/collection/all_movement_disorders">http://www.neurology.org/cgi/collection/all_movement_disorders</a> <b>All Cognitive Disorders/Dementia</b><br><a href="http://www.neurology.org/cgi/collection/all_cognitive_disorders_dementia">http://www.neurology.org/cgi/collection/all_cognitive_disorders_dementia</a> |
| <b>Permissions &amp; Licensing</b>        | Information about reproducing this article in parts (figures, tables) or in its entirety can be found online at:<br><a href="http://www.neurology.org/misc/Permissions.shtml">http://www.neurology.org/misc/Permissions.shtml</a>   |
| <b>Reprints</b>                           | Information about ordering reprints can be found online:<br><a href="http://www.neurology.org/misc/reprints.shtml">http://www.neurology.org/misc/reprints.shtml</a>   |

